

Preparation and characterisation of spherical Co/SiO₂ model catalysts with well-defined nano-sized cobalt crystallites and a comparison of their stability against oxidation with water

A.M. Saib^{a,b,*}, A. Borgna^{a,1}, J. van de Loosdrecht^b, P.J. van Berge^b, J.W. Geus^c,
J.W. Niemantsverdriet^a

^a Schuit Institut of Catalysis, Eindhoven University of Technology, P.O. Box 513, Eindhoven 5600 MB, The Netherlands

^b Sasol Technology (Pty) Ltd, P.O. Box 1, Sasolburg 1947, South Africa

^c Department of Inorganic Chemistry and Catalysis, Utrecht University, P.O. Box 80125, Utrecht 3508 TC, The Netherlands

Received 1 December 2005; revised 8 February 2006; accepted 8 February 2006

Available online 13 March 2006

Abstract

The oxidation of nanosized metallic cobalt to cobalt oxide during Fischer–Tropsch synthesis has long been postulated as a major deactivation mechanism apparently related to cobalt crystallite size. To establish a connection between cobalt crystallite size and oxidation behaviour, well-defined spherical Co/SiO₂ model catalysts with average cobalt crystallite sizes of 4, 13, and 28 nm were synthesised. The crystallite size distribution of the spherical Co/SiO₂ model catalysts was characterised with high-resolution transmission electron microscopy and in situ X-ray diffraction. The oxidation behaviour of the reduced spherical Co/SiO₂ model catalysts of differing cobalt crystallite size was studied using in situ X-ray absorption fine structure under model oxidation conditions (H₂O/He, $P_{\text{H}_2\text{O}} = 0.04$ bar). Surprisingly, it was found that the spherical Co/SiO₂ model catalyst with small cobalt crystallites (i.e., 4 nm) did not show oxidation under H₂O/He mixtures ($P_{\text{H}_2\text{O}} = 0.04$ –0.3 bar) up to 400 °C, which is against bulk thermodynamic calculations for the oxidation of cobalt metal to cobalt oxide. This was attributed to the encapsulation of the cobalt crystallites with silica after reduction at 500 °C in hydrogen. The encapsulation was verified with high-resolution transmission electron microscopy. The spherical Co/SiO₂ model catalysts with medium-sized cobalt crystallites (i.e., 13 nm) did oxidize at 100 °C and reached a maximum oxidation of 30% at 300 °C (H₂O/He; $P_{\text{H}_2\text{O}} = 0.04$ bar). The spherical Co/SiO₂ model catalysts with large cobalt crystallites (i.e., 28 nm) was found to undergo very little oxidation, <2% at 300 °C under a H₂O/He ($P_{\text{H}_2\text{O}} = 0.04$ bar) environment. In general, it could be concluded that the oxidation of spherical Co/SiO₂ model catalysts with water is difficult and is size-dependent.

© 2006 Elsevier Inc. All rights reserved.

Keywords: GTL; Fischer–Tropsch; Cobalt; Silica spheres; Deactivation; Oxidation; Water; Encapsulation; XANES; Model catalyst

1. Introduction

Fischer–Tropsch synthesis (FTS) is currently an economically attractive process for the production of environmentally friendly diesel fuel [1]. Supported cobalt catalysts are the system of choice for the FTS due to the high per pass conversion, low water–gas shift activity, and paraffinic nature of the result-

ing synthetic crude [2–5]. However, cobalt catalysts as used in the FTS are relatively expensive (compared with iron) and require a high metal dispersion and long life to remain economically feasible [6]. Hence, for the optimum cobalt usage, detailed fundamental understanding of the sensitivity of the FTS activity, selectivity, and deactivation rate to the cobalt crystallite size is imperative. Generally, most authors conclude that the FTS is a structure-insensitive reaction; that is, there are no major changes in activity and selectivity over a wide crystallite size range [7,8]. However, the oxidation of cobalt to cobalt oxide by means of water has long been postulated as a major deactivation mechanism during FTS [2,9–24] and is thought to be

* Corresponding author. Fax: +27 11 522 4488.

E-mail address: abdoool.saib@sasol.com (A.M. Saib).

¹ Present address: Institute of Chemical and Engineering Sciences, 1 Pesek Road, Jurong Island, Singapore 627833, Singapore.

related to cobalt crystallite size distribution [2,9,10,13,14,16,18–20,23,24].

Experimentally, it is difficult to find support for these threshold values, and often contradictory information is available with respect to oxidation [2,3,9–28]. Moreover, to date, no study has dealt specifically with the influence of crystallite size on the oxidation behaviour of cobalt. In the present study, in situ XANES (a powerful and sensitive technique that can differentiate between Co^0 , CoO , Co_3O_4 , and, to a lesser extent, Co_2SiO_4) was used to study the sensitivity of supported nanosized cobalt crystallites of varying sizes to oxidation by water. To facilitate detailed characterisation of the cobalt crystallites with high-resolution electron microscopy, a spherical model silica support was used. Spherical model silica supports have been used as model catalysts by Datye et al. [29,30]. The attraction in using spherical model silica supports is that it allows for the viewing of nanosized crystallites in profile with high-resolution transmission electron microscopy (HRTEM).

2. Experimental

2.1. Catalyst preparation

2.1.1. Preparation of nonporous silica spheres

The nonporous silica spheres were prepared as described previously [31]. TEOS (Merck grade), ethanol (99.9%, Merck grade), distilled water, and ammonia (25% v/v, Merck grade) were mixed in the prescribed amounts and stirred for 24 h in a conical flask. Then the silica containing slurry was dried in a rotor evaporator at 75 °C, to ensure improved handling and maximum recovery of the nonporous silica spheres after the reaction compared with separating the silica spheres by centrifugation. After drying, the silica spheres were calcined at 400 °C to remove adsorbed ammonia.

2.1.2. Preparation of spherical Co/SiO_2 model catalysts with small (<5 nm) cobalt crystallites

For the preparation of a well-defined spherical Co/SiO_2 model catalyst with nanosized (<5 nm) cobalt crystallites, the cobalt crystallites were precipitated separately from the support by adding a highly concentrated NH_3 solution to a dilute cobalt nitrate solution [32]. After 15 min of aging, the precipitate was separated from the suspension by centrifugation. The precipitate was redispersed in water and mixed with the silica support. After deposition of the precipitate onto the silica support, the 5 wt% spherical Co/SiO_2 model catalyst was calcined at 250 °C in air for 2 h and reduced at 450 °C for 4 h in 1 bar pure hydrogen (H_2 purity = 5.0) unless otherwise indicated. This catalyst is referred to as Co-4nm hereinafter.

2.1.3. Preparation of spherical Co/SiO_2 model catalysts with medium-sized (ca. 10 nm) cobalt crystallites

A well-defined spherical Co/SiO_2 model catalyst with cobalt crystallites of ca. 10 nm was prepared by means of “impregnation,” that is, mixing an aqueous cobalt nitrate solution with the nonporous silica spheres so as to produce a 10 wt% Co/SiO_2 model catalyst. (Note that true impregnation is possible only in

the presence of pores, hence the quotation marks.) After this impregnation, the 10 wt% spherical Co/SiO_2 model catalyst was dried in a rotor evaporator at 75 °C, calcined at 250 °C in air for 2 h, and reduced at 450 °C for 4 h in 1 bar pure hydrogen (H_2 purity = 5.0) unless otherwise indicated. This catalyst is referred to as Co-13nm hereinafter.

2.1.4. Preparation of spherical Co/SiO_2 model catalysts with large (>15 nm) cobalt crystallites

For the preparation of a well-defined spherical Co/SiO_2 model catalyst with cobalt crystallites >15 nm, the impregnation method as outlined above was applied using dehydroxylated silica spheres obtained from Degussa (Aerosil, OX 50). After impregnation, the 10 wt% spherical Co/SiO_2 model catalyst was calcined at 250 °C in air for 2 h and reduced at 450 °C for 4 h in 1 bar pure hydrogen (H_2 purity = 5.0) unless otherwise indicated. This catalyst is referred to as Co-28nm hereinafter.

2.2. Catalyst characterisation

2.2.1. HRTEM

HRTEM measurements were carried out on reduced cobalt samples that had been passivated in a glove box ($\text{O}_2 = 1$ ppm and $\text{H}_2\text{O} = 1$ ppm). For determination of the cobalt crystallite size distributions, only samples that had been completely reoxidised in air were used. Thin samples for HRTEM were prepared by crushing the spherical Co/SiO_2 model catalyst with a mortar and pestle, followed by dispersion in ethanol using an ultrasound bath. Then an appropriate amount of sample was placed onto a copper microscope grid covered with carbon windows. Samples were studied using a Philips/Fei Tecnai 20F high-resolution microscope with an acceleration voltage of 200 keV. To compare oxidised Co_3O_4 metal crystallite sizes obtained from TEM with the metallic cobalt crystallite sizes obtained from in situ XRD, Co_3O_4 crystallite sizes were converted to the corresponding metallic crystallite sizes according to the relative molar volumes of metallic cobalt and Co_3O_4 [33]. The conversion factor for the diameter of a given Co_3O_4 crystallite being reduced to metallic cobalt is

$$d(\text{Co}^0) = 0.75d(\text{Co}_3\text{O}_4).$$

To determine the cobalt crystallite size distribution and their average size, >250 cobalt crystallites were counted for each sample. The average size was determined using the following formula:

$$dv = \frac{\sum n_i d_i^4}{\sum n_i d_i^3}.$$

Dispersions of the spherical model catalysts were calculated from the average cobalt crystallite size assuming spherical uniform cobalt crystallites with a site density of 14.6 atoms/nm² using the following formula [34]:

$$D (\%) = 96/d_{\text{nm}}.$$

2.2.2. *In situ* XRD

In situ XRD measurements were performed on a dynamic X-ray diffractometer (DXRD). Approximately 0.15 ml of the spherical Co/SiO₂ model catalyst was packed in the DXRD sample holder. The X-ray generator was operated at 40 kV and 40 mA, using a 1.8 kW long fine-focus cobalt tube. Scans were done in continuous mode using a step size of 0.0167° 2 θ and a counting time of 0.248 s per step. The scanning range was 5–105° 2 θ , with 20 min per scan. During measurement, a gas flow rate of 100 ml (NTP)/min hydrogen was used at atmospheric pressure. The temperature was increased in 20 °C increments from 100 to 420 °C, with a scan recorded at each 20 °C interval. Subsequently, the temperature was increased to 425 °C, followed by four scans with a waiting period of 1 h between scans. The peaks on the diffractograms were identified by means of the Joint Committee on Powder Diffraction (JCPDS) database [35]. Average cobalt crystallite sizes were determined using Scherrer's equation [36] using the Co (111) peak for Co metal, the Co (311) peak for Co₃O₄, and the Co (111) and Co (200) peaks for CoO. Peak half-widths were obtained directly from the diffractograms. α -Alumina was used as an external standard to correct for instrumental broadening.

2.2.3. Temperature-programmed reduction

The calcined spherical Co/SiO₂ model catalyst was loaded into a quartz temperature-programmed reduction (TPR) cell and dried at 250 °C (at a rate of 5 °C/min) in N₂ for 2 h. A drying step was used to remove all adsorbed water. Subsequently, the reactor was cooled to 25 °C. Thereafter, the catalyst was reduced using a linear temperature program (at a rate of 10 °C/min to 800 °C) in 5% H₂/N₂.

2.2.4. *In situ* XANES analyses of spherical model catalysts

XANES measurements on Co⁰, CoO, Co₃O₄, and Co₂SiO₄ reference compounds and spherical Co/SiO₂ model catalysts were performed at the Lure synchrotron center (ORSAY-France) using a beam line with energy of 1.85 GeV. A Si (111) monochromator was used to vary the energy within the desired range. Measurements were carried out at the *K*-edge of Co. Calibration was performed with a Co foil using the first point of inflection of Co, that is, 7709 eV [37].

The reactor used for *in situ* measurements was similar to the one designed by Lytle et al. [38,39]. Spherical model catalysts

were reduced *in situ* using a H₂ flow rate of 25 ml (NTP)/min while heating to the desired temperature. Spectra were acquired every 20–60 °C, depending on the heating rate. Model oxidation experiments were carried out with a ca. 25 ml (NTP)/min H₂O/He flow ($P_{\text{H}_2\text{O}} = 0.04\text{--}0.3$ bar) while heating to 400 °C. All gas lines between the saturator and reactor were heated, to prevent condensation of the water vapour. The operation of the saturator was verified with a mass spectrometer. Gases used were all ultra-pure (99.999% purity).

The XANES spectra were extracted from raw data by a conventional procedure. The pre-edge background was subtracted using power series curves. Subsequently, the spectra were normalized by dividing by the height of the absorption edge. Spectra were quantified by fitting the experimental data with a weighted linear combination of reference compounds (Co⁰, CoO, Co₃O₄, and Co₂SiO₄).

2.2.5. Attenuated total reflection infrared spectroscopy (ATR-IR)

A Nicolet Protege 460 Fourier transform infrared spectrometer with a Nicolet Smart Golden Gate Mk II total reflectance device was used to scan the 4000–650 cm⁻¹ region, with 32 scans and a 2 cm⁻¹ resolution.

3. Results

3.1. Catalyst preparation and characterisation

Fig. 1 shows low-resolution scanning electron microscopy (SEM) images of the synthesised silica spheres used as a model silica support for subsequent catalyst preparations. After drying, the spherical model silica support is a fluffy agglomeration of individual silica spheres of ca. 100–200 nm diameter.

Fig. 2 shows HRTEM images of the synthesised silica spheres. The silica spheres were nonporous and smooth-surfaced with sharp edges, facilitating subsequent electron microscopy.

The preparation of well-defined supported nanosized cobalt crystallites in the range reported for oxidation [2,23,24] (i.e., 5–10 nm) is difficult using a simple impregnation, that is, mixing a cobalt nitrate solution with the nonporous silica spheres followed by drying. Hence, a controlled precipitation of cobalt nitrate with ammonia followed by the deposition of the precip-

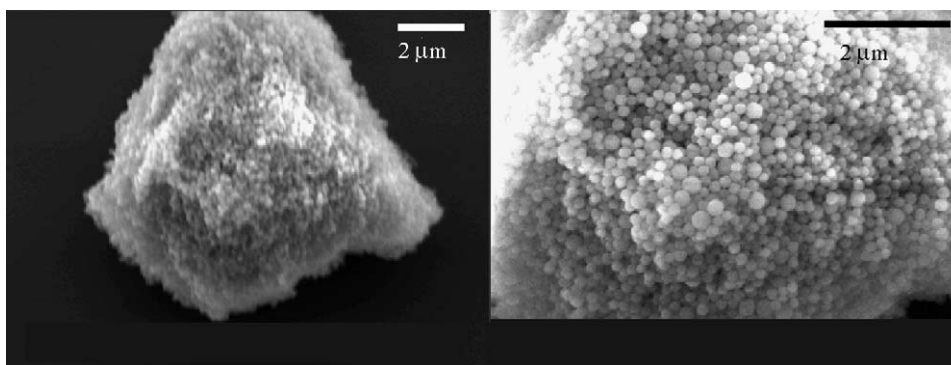


Fig. 1. Secondary electron microscopy (SEM) images of the synthesised silica spheres.

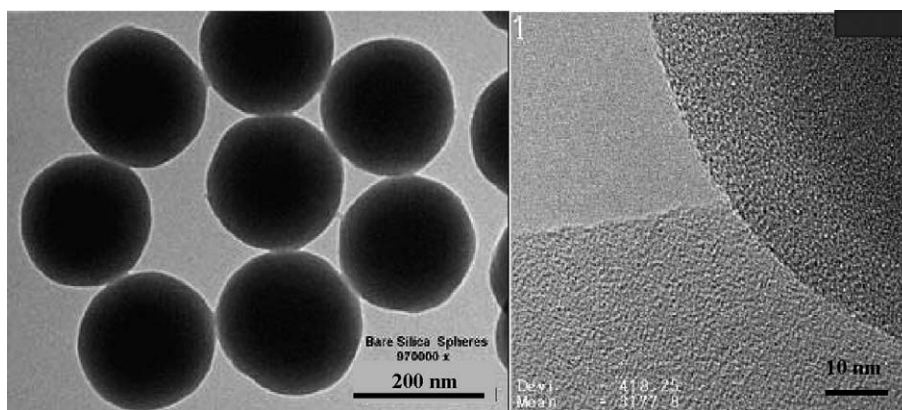


Fig. 2. Transmission electron microscopy images of the synthesised silica spheres.

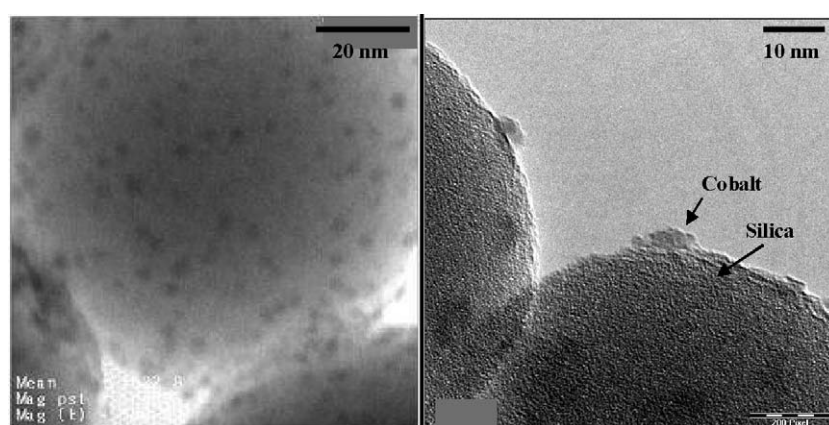


Fig. 3. Transmission electron microscopy images of a 5 wt% Co/SiO₂ spherical model catalyst (Co-4nm) prepared by “deposition” precipitation followed by calcination in air at 250 °C and reduction in pure hydrogen at 425 °C. Samples following reduction were passivated in a glove box (O₂ = 1 ppm and H₂O = 1 ppm).

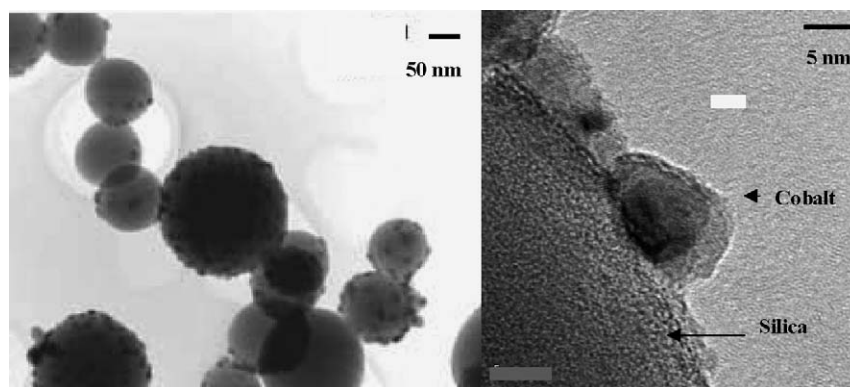


Fig. 4. Transmission electron microscopy images of a 10 wt% spherical model Co/SiO₂ catalyst (Co-13nm) prepared by “impregnation” followed by calcination in air at 250 °C and reduction in pure hydrogen at 425 °C. Samples following reduction were passivated in a glove box (O₂ = 1 ppm and H₂O = 1 ppm).

itate onto the nonporous silica spheres was used to prepare a 5 wt% Co/SiO₂ spherical model catalyst. The cobalt loading for the synthesis of nanosized cobalt crystallites is limited by the low surface area of the silica spheres. A monolayer coverage of the silica spheres (100 nm) with cobalt corresponds to a 5–6 wt% Co/SiO₂ loading. Fig. 3 shows TEM images of the 5 wt% Co/SiO₂ spherical model (Co-4nm) catalyst prepared by deposition precipitation followed by calcination in air at 250 °C and reduction in pure hydrogen at 425 °C. The resulting 5 wt% Co/SiO₂ spherical model catalyst was found to be extremely

homogeneous and well defined, with a narrow cobalt crystallite size distribution of 3–4 nm. Fig. 7 summarises the metallic cobalt crystallite size distribution, corrected for oxidation, as obtained from TEM.

For the preparation of medium-sized (i.e., ca. 10 nm) cobalt crystallites on the spherical model silica support, an impregnation method was applied, that is, mixing a cobalt nitrate solution with the hydroxylated nonporous silica spheres followed by drying. Fig. 4 shows TEM images of the 10 wt% Co/SiO₂ spherical model catalyst (Co-13nm) prepared by impregnation

followed by calcination in air at 250 °C and reduction in pure hydrogen at 425 °C. The resulting 10 wt% Co/SiO₂ spherical model catalyst was fairly homogenous, with a cobalt crystallite size distribution of 8–15 nm. The absence of cobalt crystallites on some of the silica spheres (Fig. 4) is most likely due to the microagglomeration (Fig. 1) of silica spheres after support preparation, which prevents the deposition of cobalt on each silica sphere during impregnation. During sample preparation for TEM, the spherical model Co/SiO₂ catalyst was thoroughly crushed, exposing the silica spheres from within the agglomerates. Fig. 7 summarises the metallic cobalt crystallite size distribution of the 10 wt% Co/SiO₂ spherical model catalyst, corrected for oxidation, as obtained from TEM.

To further increase the cobalt crystallite size (i.e., to produce spherical Co/SiO₂ model catalysts with cobalt crystallites >15 nm), a dehydroxylated spherical model silica support obtained from Degussa (Aerosil OX 50) was used. Fig. 5 shows an ATR-IR spectrum of the dehydroxylated Degussa spherical model silica support as compared to that of the in-house-synthesised nonporous silica spheres. The absence of the silanol peak [40] at 3740 cm⁻¹ confirms the dehydroxylated nature of the Degussa spherical model silica support compared with the in-house-synthesised nonporous silica spheres. This absence of

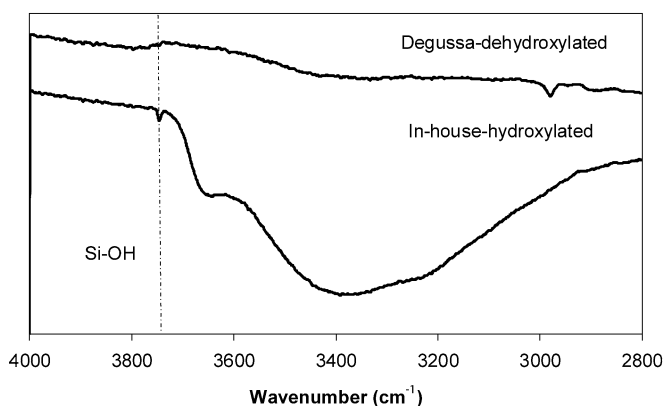


Fig. 5. Attenuated total reflection (ATR-IR) analyses of the dehydroxylated spherical model silica support obtained from Degussa (Aerosil OX 50) and the “in house” synthesised nonporous silica spheres.

silanol groups creates a hydrophobic spherical model silica support, as indicated on ATR-IR by the lack of adsorbed water (absence of water peak between 3000 and 3600 cm⁻¹ [40]), which minimises the interaction between the surface of the silica spheres and the cobalt nitrate precursor during impregnation. Fig. 6 shows TEM images of the 10 wt% spherical model Co/SiO₂ (Degussa) catalyst (Co-28nm) prepared by impregnation of a dehydroxylated model silica support obtained from Degussa, followed by calcination in air at 250 °C and reduction in pure hydrogen at 425 °C. This catalyst was inhomogeneous, due to the nature of the support. Fig. 7 summarises the metallic cobalt crystallite size distribution, corrected for oxidation, as obtained from TEM.

The crystallite size distributions of the spherical Co/SiO₂ model catalysts of varying cobalt crystallite sizes were also corroborated using in situ dynamic X-ray diffraction (D-XRD). With in situ D-XRD, Scherrer’s equation was used to determine the average metallic cobalt crystallite size of the spherical Co/SiO₂ model catalysts after reduction at 425 °C under hydrogen. Table 1 summarises the crystallite size distributions for the reduced spherical Co/SiO₂ model catalysts obtained from in situ D-XRD and ex situ TEM. A good agreement was found between D-XRD and TEM after correction for the oxidation state of cobalt.

3.2. XANES study of the reduction behaviour of the spherical Co/SiO₂ model catalysts of varying cobalt crystallite size

To understand the influence of the cobalt crystallite size on the reduction behaviour of the spherical Co/SiO₂ model catalysts, X-ray absorption near-edge spectroscopy (XANES) was used. Before this, XANES spectra of all relevant cobalt reference compounds (i.e., Co⁰, CoO, Co₃O₄, and Co₂SiO₄) were obtained (Fig. 8). Fig. 8 shows that all oxidic reference compounds display a strong absorption white line (ca. 7730 eV), with subsequent differences in the spectra for CoO/Co₂SiO₄ and Co₃O₄ due to the existence of cobalt ions in different Co–O environments and oxidation states. It is clear from Fig. 8 that XANES makes it easy to distinguish among Co⁰, CoO, Co₃O₄, and, to a lesser extent, Co₂SiO₄.

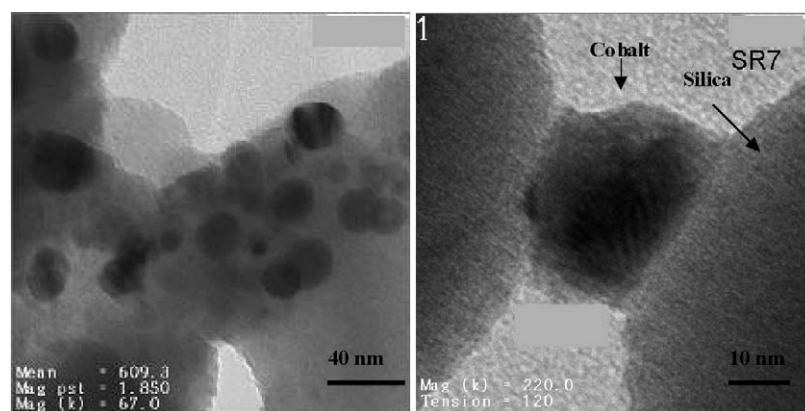


Fig. 6. Transmission electron microscopy images of a 10 wt% spherical model Co/SiO₂ (Degussa) catalyst (Co-28nm) prepared by “impregnation” of a dehydroxylated model silica support obtained from Degussa followed by calcination in air at 250 °C and reduction in pure hydrogen at 425 °C. Samples following reduction were passivated in a glove box (O₂ = 1 ppm and H₂O = 1 ppm).

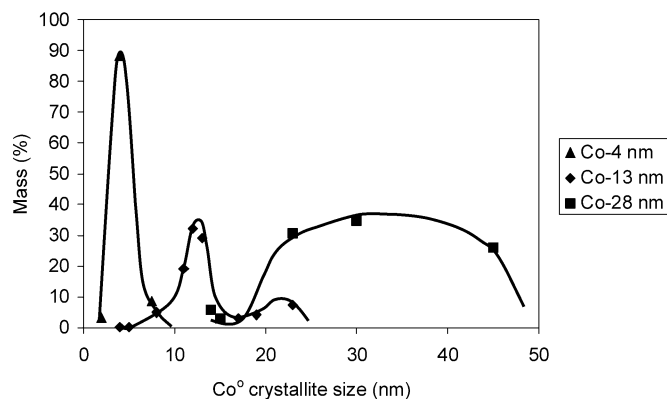


Fig. 7. Metallic cobalt crystallite size distribution for spherical Co/SiO₂ model catalysts obtained with TEM. (▲) Co-4nm: 5 wt% Co/SiO₂ spherical model catalyst prepared by deposition precipitation; (◆) Co-13nm: 10 wt% spherical model Co/SiO₂ catalyst prepared by “impregnation”, i.e., mixing of a cobalt nitrate solution with the non-porous silica spheres followed by drying; (■) Co-28nm: 10 wt% spherical model Co/SiO₂ (Degussa) catalyst prepared by “impregnation” of dehydroxylated model silica support obtained from Degussa. All spherical model catalysts were calcined in air at 250 °C and reduced in pure hydrogen at 425 °C.

Table 1

Crystallite size distributions of reduced spherical Co/SiO₂ model catalysts of differing cobalt crystallite size using in situ D-XRD and ex situ TEM. The crystallite sizes were corrected for the oxidation state of cobalt

Catalyst	Metallic cobalt crystallite size (nm)	
	TEM	In situ D-XRD
Co-4nm	4	4
Co-13nm	13	Not measured
Co-28nm	30	25

Figs. 9a–c show the reduction of spherical Co/SiO₂ model catalysts with large cobalt crystallites (Co-28nm; in situ reduction conditions: rate of 5 °C/min to 450 °C in pure hydrogen with a spectrum measured ca. every 60 °C), medium cobalt crystallites (Co-13nm; in situ reduction conditions: rate of 5 °C/min to 450 °C in pure hydrogen with a spectrum measured ca. every 60 °C), and small cobalt crystallites (Co-4nm; in situ reduction conditions: rate of 2 °C/min to 150 °C with a spectrum measured ca. every 20 °C and a rate of 3 °C/min to 150–450 °C with a spectrum measured every 30 °C), as followed by XANES. The spherical Co/SiO₂ model catalysts with cobalt crystallites >8 nm (Co-13nm and Co-28nm) contained mainly cobalt in the Co₃O₄ phase after calcination at 250 °C. Cobalt present in the spherical Co/SiO₂ model catalyst with small cobalt crystallites (Co-4nm) was largely a mixture of CoO and Co₂SiO₄ after calcination. The similar XANES spectra of CoO and Co₂SiO₄ makes it difficult to resolve the mixture into separate components of CoO and Co₂SiO₄. The spherical Co/SiO₂ model catalysts Co-13nm and Co-28nm were found to reduce in two steps, Co₃O₄ to CoO (ca. 290–320 °C) and CoO to cobalt metal (ca. 320–450 °C). Whereas the spherical Co/SiO₂ model catalyst with small cobalt crystallites (Co-4nm) showed a large one-step reduction from CoO to cobalt metal (ca. 400–500 °C). The reduction of Co₂SiO₄ is not expected at such low temperatures [41].

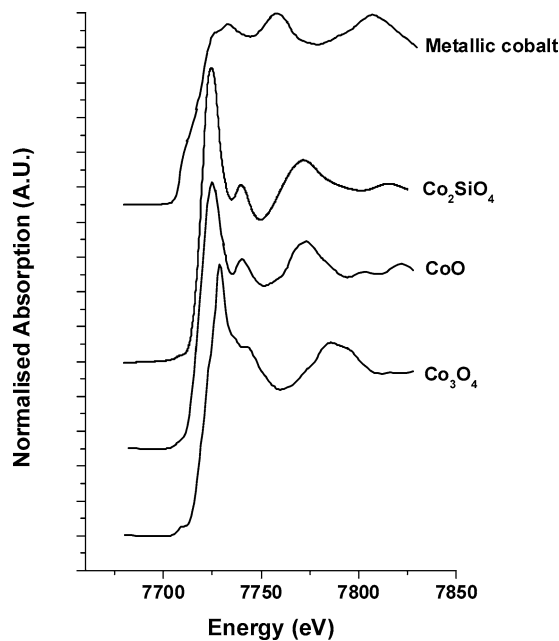


Fig. 8. XANES analyses of cobalt reference compounds Co⁰, CoO, Co₃O₄, and Co₂SiO₄.

To obtain a quantitative description of the degree of reduction of the spherical Co/SiO₂ model catalysts of varying cobalt crystallite size, a weighted linear combination of the reference compounds (Fig. 8) was used. The spherical Co/SiO₂ model catalysts with large cobalt crystallites (Co-13nm and Co-28nm) reduced readily and had a 89% reduction of Co⁰ in Co-13nm and a 95% reduction of Co⁰ in Co-28nm at 450 °C. The spherical model catalyst with small cobalt crystallites (Co-4nm) had a 65% degree of reduction at 500 °C.

3.3. TPR study of the spherical Co/SiO₂ model catalysts of varying cobalt crystallite size

The influence of cobalt crystallite size on the reduction behaviour of the Co/SiO₂ spherical model catalysts was further studied with TPR. Fig. 10 shows the TPR spectra of the 5 wt% Co/SiO₂ spherical model catalyst with small cobalt crystallites (Co-4nm), the 10 wt% Co/SiO₂ spherical model catalyst with medium-sized cobalt crystallites (Co-13nm), and the 10 wt% Co/SiO₂ spherical model catalyst with large cobalt crystallites (Co-28nm). The spherical Co/SiO₂ model catalysts with large cobalt crystallites (Co-13nm and Co-28nm) were found to undergo a two-step reduction ascribed to the reduction of Co₃O₄ to CoO [peak 1, Eq. (1)] and of CoO to cobalt metal [peak 2, Eq. (2)] [41]. This is supported by the ratio of the area of the second TPR peak and the area of the first TPR peak, which is close to the stoichiometric hydrogen consumption ratio of 3 for the two-step reduction of Co₃O₄ to cobalt metal (Table 2),



The small peak at ca. 80 °C (peak 1a) is most likely due to the reduction of residual cobalt nitrate after calcination. The

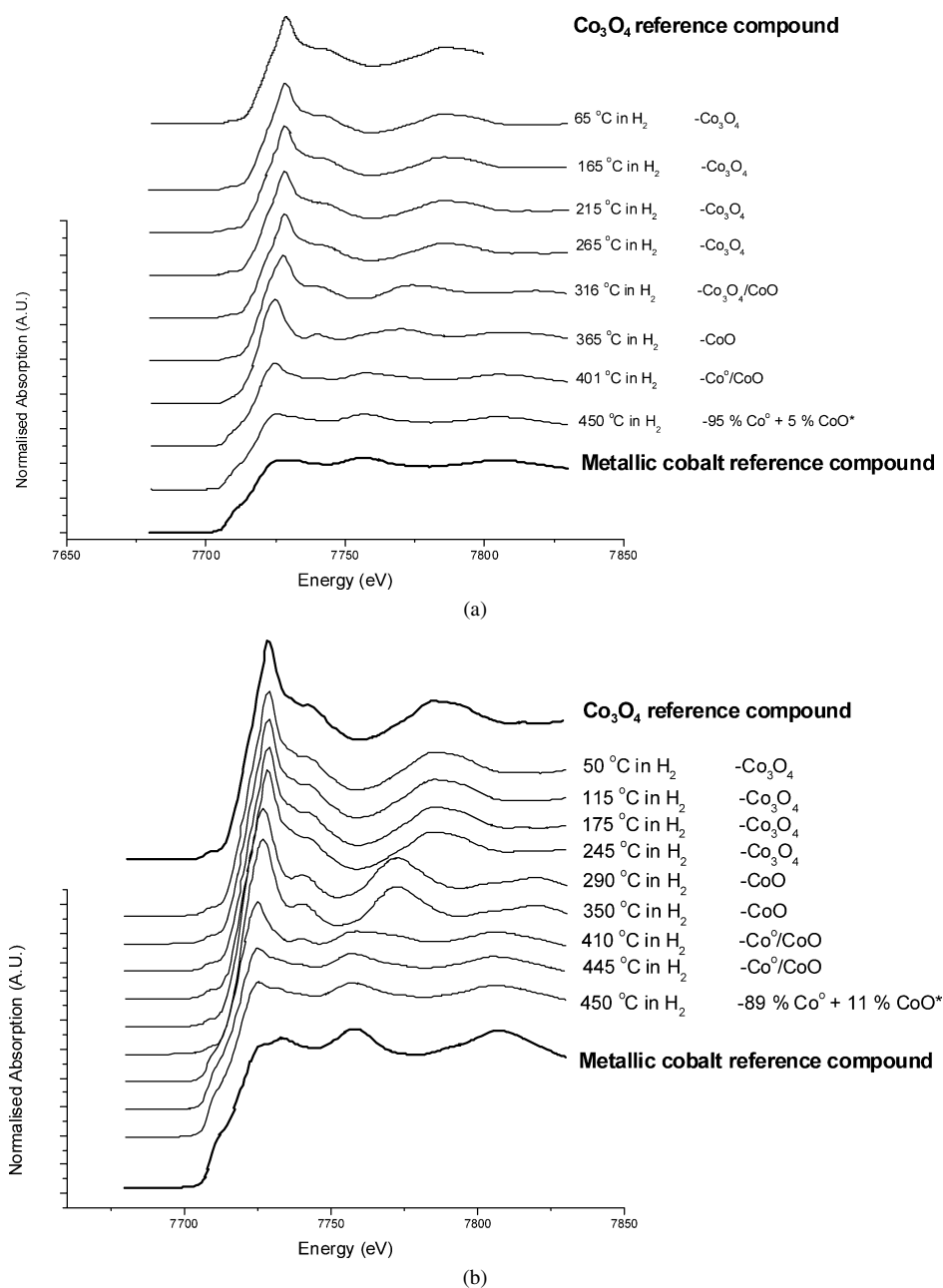


Fig. 9. Reduction of 10 wt% Co/SiO₂ spherical model catalyst with large (Co-28nm) (a), medium sized (Co-13nm) (b), and small (Co-4nm) (c) cobalt crystallites following calcination at 250 °C in air. Reduction conditions: (a,b) 5 °C/min to 450 °C in pure hydrogen with a spectrum measured every ca. 60 °C (* minor cobalt silicate cannot be ruled out), (c) 2 °C/min to 150 °C with a spectrum measured every ca. 20 °C and 150–450 °C at 3 °C/min with a spectrum measured every 30 °C (for clarity every second spectrum is shown).

spherical Co/SiO₂ model catalyst with small cobalt crystallites (Co-4nm) also showed two reduction peaks. The reduction steps were shifted to higher temperatures, with the first peak at around 300 °C and the second peak at around 540 °C. The first peak is attributed to the reduction of a small amount of Co₃O₄ to CoO. The second peak is much larger than the first peak, and the ratio between the areas of the two peaks is now 8.5. This second peak is attributed to the one-step reduction of CoO to cobalt metal due to the fact that the reduction of Co₃O₄ occurs at lower temperatures and that of cobalt silicate occurs at much higher reduction temperatures (i.e., above 800 °C) [41]. The shoulder at 700 °C is most likely due to the reduction of cobalt

silicate-like species. Table 2 summarises the areas and positions of the peaks in the TPR spectra of the spherical Co/SiO₂ model catalysts with varying cobalt crystallite sizes. The temperatures of the maximum of the first and second peaks in the TPR spectrum were found to increase with decreasing cobalt crystallite size.

3.4. Dynamic in situ XRD study of the spherical Co/SiO₂ model catalysts of varying cobalt crystallite size

The resulting cobalt phases for the spherical Co/SiO₂ model catalysts with large (Co-28nm) and small (Co-4nm) cobalt

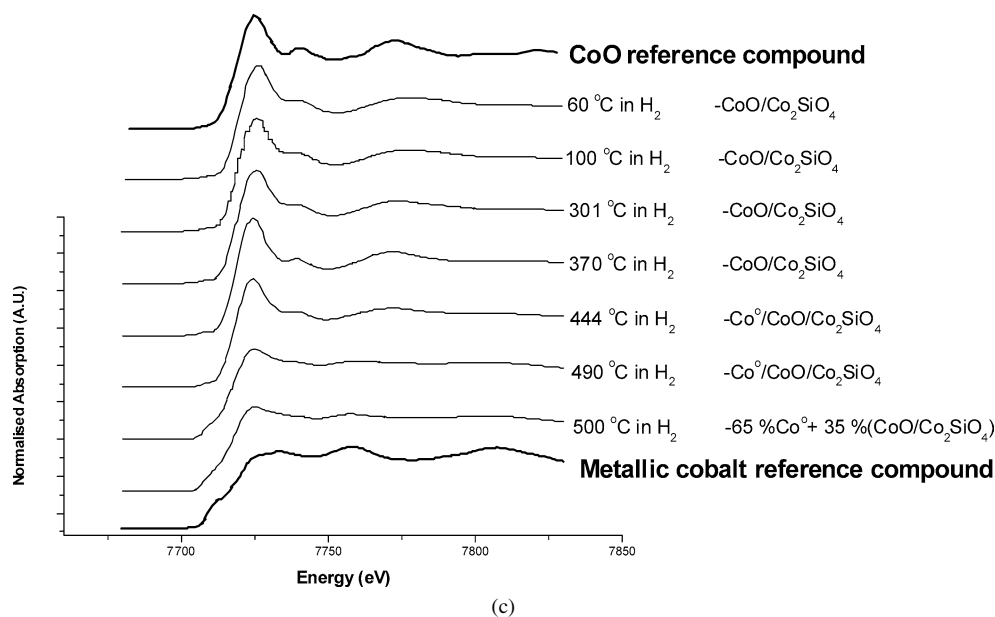


Fig. 9. (continued)

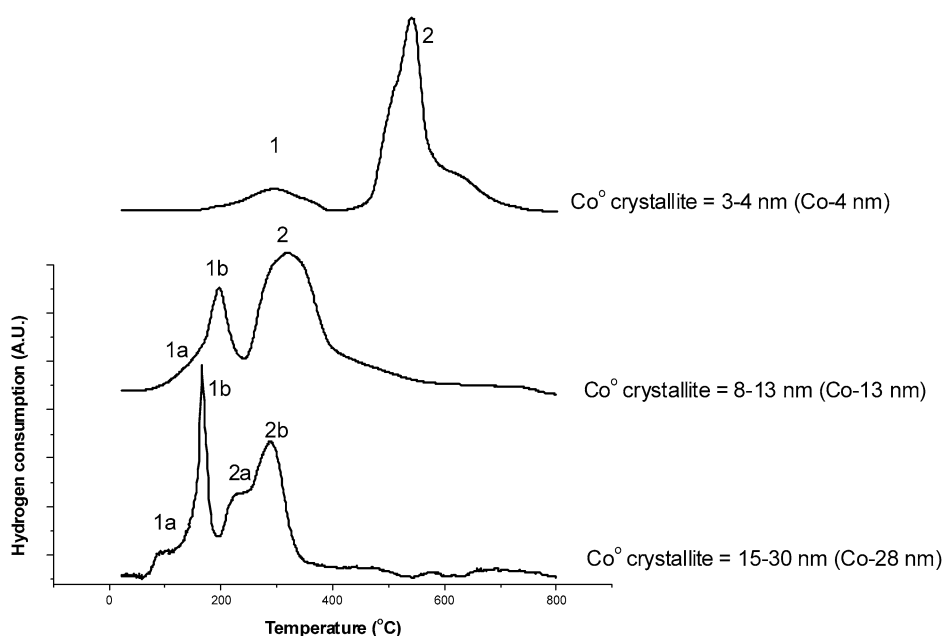


Fig. 10. TPR spectra of (a) spherical Co/SiO₂ model catalyst with large cobalt crystallites (Co-28nm) following calcination (b) spherical Co/SiO₂ model catalyst with medium cobalt crystallites (Co-13nm) following calcination and (c) spherical Co/SiO₂ model catalyst with small cobalt crystallites (Co-4nm) following calcination TPR conditions: 5% H₂/N₂, 25–800 °C, 10 °C/min.

Table 2

TPR peak positions and areas for the reduction of spherical model catalysts of varying cobalt crystallite sizes

	Co/SiO ₂ (Co-4nm)		Co/SiO ₂ (Co-13nm)		Co/SiO ₂ (Co-28nm)	
	Peak 1	Peak 2	Peak 1	Peak 2	Peak 1	Peak 2
T _{max} (°C)	297	542	200	326	166	287
Ratio peak 2/peak 1	8.5		2.9		2.8	

crystallites after reduction (rate of 1 °C/min to 425 °C in pure hydrogen), that is, cubic or hexagonal cobalt, was studied using D-XRD. The spherical 10 wt% Co/SiO₂ model catalyst with large cobalt crystallites (Co-28nm) after calcination in air at

250 °C was mainly Co₃O₄ (Fig. 11a), in agreement with the XANES findings. The spherical 5 wt% Co/SiO₂ model catalyst with small cobalt crystallites (Co-4nm) was found to display no signal after calcination, due to the size and amorphous nature

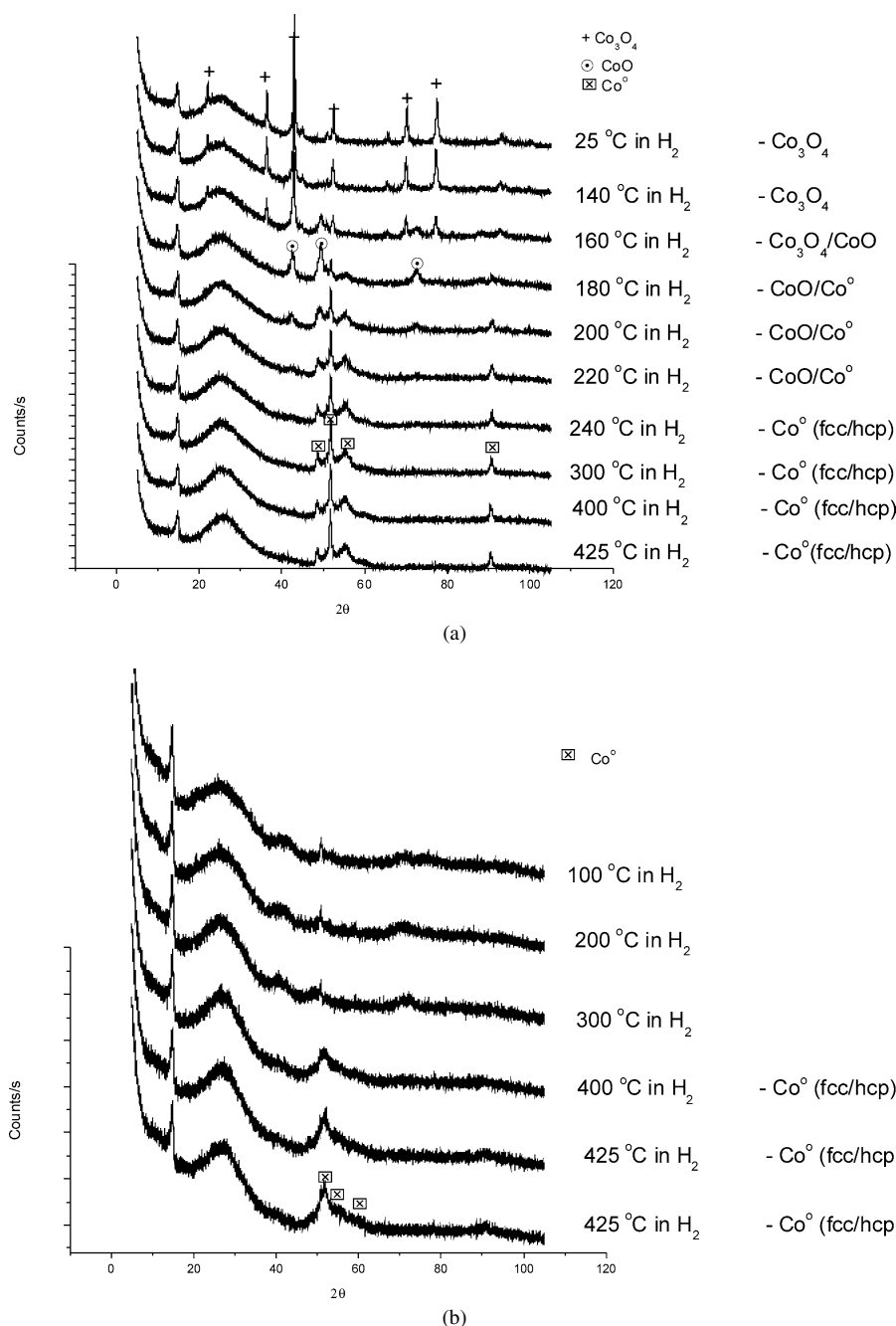


Fig. 11. In situ D-XRD analyses of the reduction of a spherical Co/SiO₂ model catalyst with (a) large cobalt crystallites (Co-28nm) and (b) small cobalt crystallites (Co-4nm) following calcination. Reduction conditions: 1 °C/min to 425 °C with a spectrum taken every 20 °C from 100 to 420 °C and every 1 h for 4 h at 425 °C.

of the cobalt crystallites (Fig. 11b) after deposition precipitation and calcination. The spherical 10 wt% Co/SiO₂ model catalyst with large cobalt crystallites (Co-28nm) was found to undergo reduction from Co₃O₄ to CoO at 160 °C and from CoO to Co metal at 200 °C (Fig. 11a). The reduction behaviour of the spherical 5-wt% Co/SiO₂ model catalyst with small cobalt crystallites (Co-4nm) was difficult to follow because of the amorphous nature of the sample (Fig. 11b). At 425 °C, XRD peaks were observed for the small cobalt crystallites corresponding to the cubic and hexagonal cobalt structure (Fig. 11b), indicating a mixture of the two phases. The spherical 10 wt% Co/SiO₂

model catalyst with large cobalt crystallites (Co-28nm) was also found to be a mixture of cubic and hexagonal cobalt after reduction at 425 °C (Fig. 11a).

3.5. In situ XANES study of the oxidation behaviour of spherical Co/SiO₂ model catalysts of varying cobalt crystallite size under model conditions

The oxidation behaviour of the spherical Co/SiO₂ model catalysts of varying cobalt crystallite size (i.e., Co-4nm, Co-13nm, and Co-28nm) was studied using in situ XANES. The model catalysts were reduced in situ (see Fig. 9). Subsequently, each

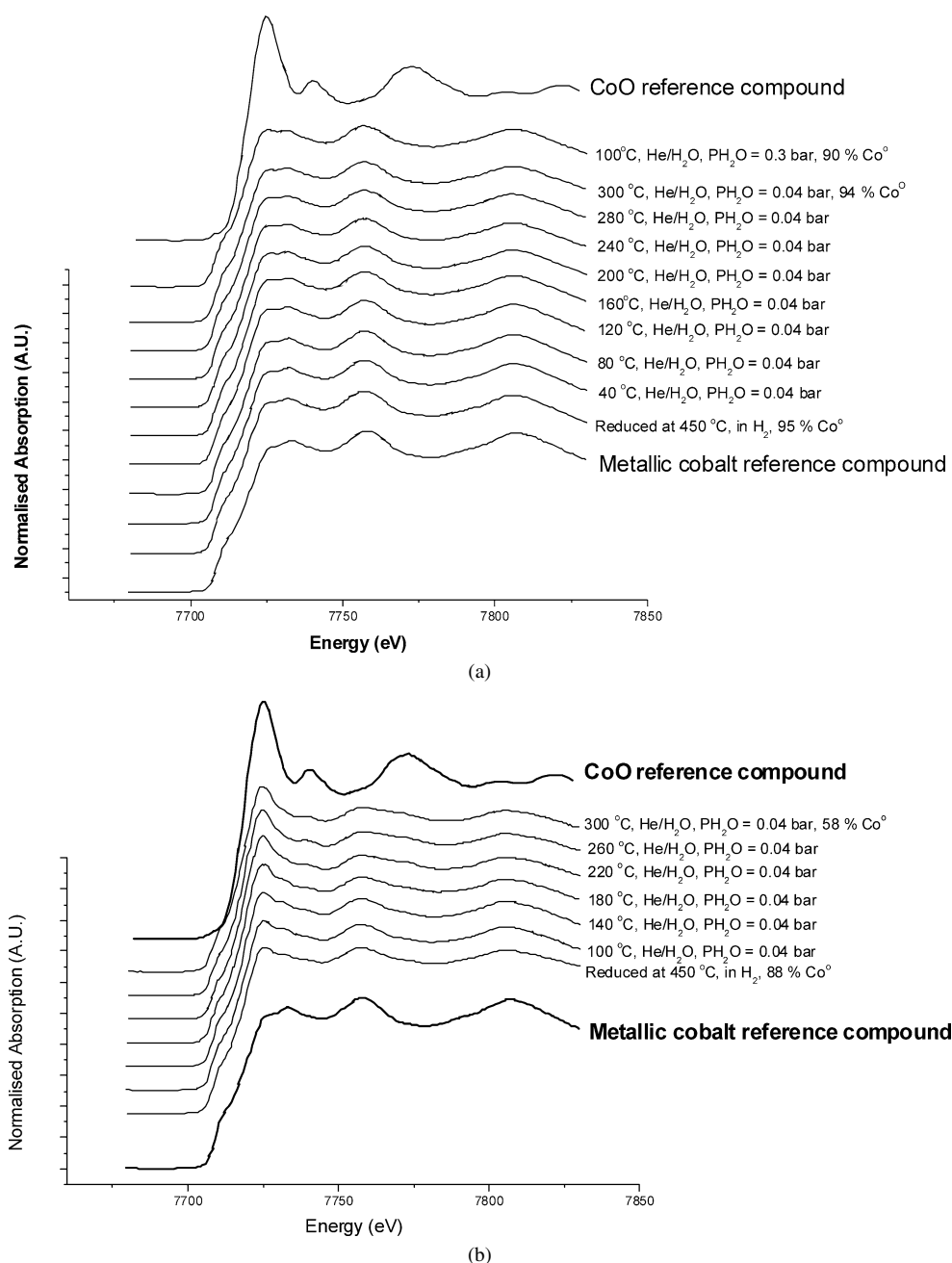


Fig. 12. Model oxidation study of spherical Co/SiO₂ model catalyst with (a) large cobalt crystallites (Co-28nm), (b) medium cobalt crystallites (Co-13nm), and (c) small cobalt crystallites (Co-4nm). In situ model oxidation conditions: 2 °C/min to 300 °C in H₂O/He ($P_{\text{H}_2\text{O}} = 0.04\text{--}0.3$ bar (a,c), 0.04 bar (b)) with a spectrum measured every ca. 40 °C.

spherical Co/SiO₂ model catalyst of varying cobalt crystallite size was exposed to a model oxidation environment (in situ model oxidation conditions: rate of 2 °C/min to 300–400 °C in H₂O/He ($P_{\text{H}_2\text{O}} = 0.04\text{--}0.3$ bar) with a spectrum measured ca. every 40 °C). The spherical Co/SiO₂ model catalyst with large cobalt crystallites (Co-28nm) was found to undergo little oxidation (i.e., <2%) up to 300 °C in a H₂O/He ($P_{\text{H}_2\text{O}} = 0.04$ bar) environment (Fig. 12a). On increasing the water partial pressure to 0.3 bar at 100 °C, slightly greater oxidation (5%) was observed. In general, the spherical Co/SiO₂ model catalyst with large cobalt crystallites (Co-28nm) was difficult to oxidise with water. The spherical Co/SiO₂ model catalyst with medium-

sized cobalt crystallites (Co-13nm) was found to undergo significant oxidation at 100 °C and reached a maximum of 30% oxidation at 300 °C in a H₂O/He ($P_{\text{H}_2\text{O}} = 0.04$ bar) environment (Fig. 12b). Surprisingly, the spherical Co/SiO₂ model catalyst with small cobalt crystallites (Co-4nm) was found to undergo no oxidation up to 400 °C (H₂O/He, $P_{\text{H}_2\text{O}} = 0.04$ bar) (Fig. 12c) even at higher water partial pressures (0.3 bar).

Because oxidation was expected from bulk thermodynamics [3], it was hypothesised that the lack of oxidation of the spherical Co/SiO₂ model catalyst with small cobalt crystallites (Co-4nm) was due to encapsulation of the cobalt crystallites with silica. An attempt was made to verify this encapsulation

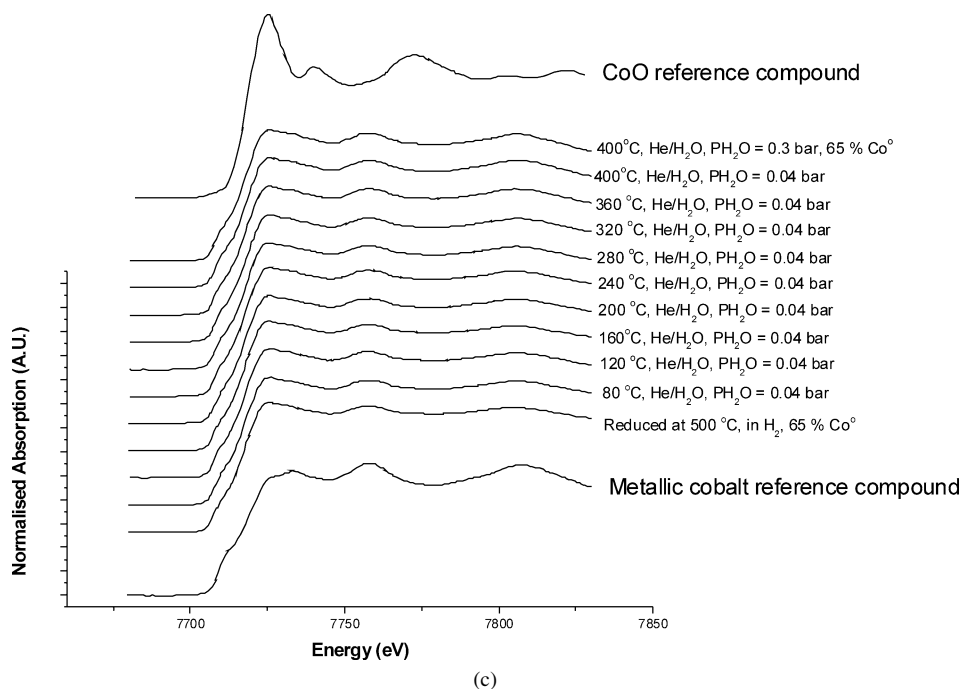


Fig. 12. (continued)

hypothesis using HRTEM. The 5 wt% Co/SiO₂ spherical model catalyst prepared by deposition precipitation (calcined in air at 250 °C) was reduced in pure hydrogen at 500 °C. However, HRTEM revealed no encapsulation of the cobalt crystallite with silica at this reduction temperature, most likely due to the presence of a monolayer of silica, which is difficult to establish with TEM. Hence, to facilitate observation of the encapsulation (i.e., by thickening the silica layer), the reduction temperature of the spherical Co/SiO₂ model catalyst with small cobalt crystallites (Co-4nm) was increased to 700 °C. Subsequently, a thick layer of amorphous silica around the cobalt crystallites could be observed with TEM (Fig. 13), indicating that silica can undergo migration during reduction and is most likely responsible for the stability of the nanosized cobalt crystallites against oxidation. Because of the encapsulation of the small cobalt crystallites (Co-4nm) with silica, relevant oxidation studies carried out under model FTS conditions (i.e., $P_{\text{H}_2\text{O}}/P_{\text{H}_2} = 1$) had no impact. Hence, whether small cobalt crystallites can deviate from bulk-phase thermodynamics cannot be determined.

4. Discussion

Table 3 summarises the physiochemical properties of the spherical model catalyst of varying Co crystallite size.

4.1. Influence of cobalt crystallite size on the reduction behaviour of Co/SiO₂ spherical model catalysts

The spherical Co/SiO₂ model catalysts following preparation and calcination were characterised with XRD, XANES, and TPR to establish a relationship between cobalt crystallite size and the resulting calcined and reduced states. The spherical Co/SiO₂ model catalyst with small cobalt crystallites (Co-4nm)

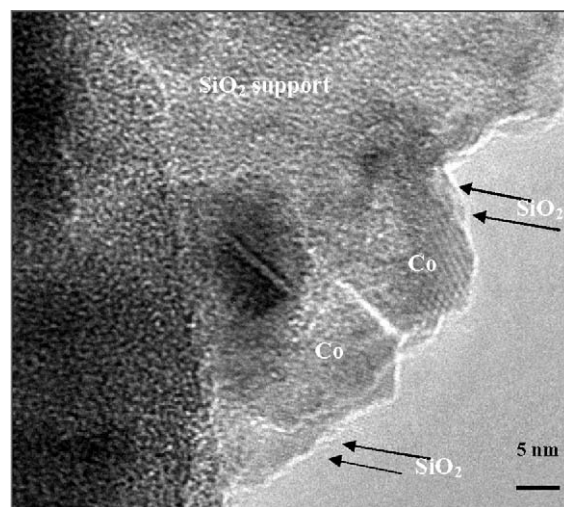


Fig. 13. TEM analyses of the spherical 5 wt% Co/SiO₂ model catalyst with small cobalt crystallites (Co-4nm) following reduction at 700 °C in pure hydrogen (arrows indicate silica migration).

was found to be largely in an amorphous CoO and Co₂SiO₄ state after calcination (XANES, TPR) and to undergo an essentially one-step reduction at ca. 400–500 °C. The difference in the onset of cobalt oxide reduction among XRD, XANES, and TPR is due to differences in the reduction conditions (i.e., heating rate, hydrogen space velocity, and hydrogen concentration). The amorphous state of cobalt catalysts prepared by precipitation with ammonia was reported previously [42]. The ratio between CoO and Co₂SiO₄, for the spherical model catalyst with small cobalt crystallites is difficult to quantify with XANES, due to the similarity of the CoO and Co₂SiO₄ spectra. However, based on the 65% degree of reduction at 500 °C (XANES), the remainder of the unreduced cobalt can be as-

Table 3
Physicochemical properties of spherical Co/SiO₂ model catalysts of varying cobalt crystallite size

Co size ^a (nm)	Dispersion ^b (%)	Calcined phase ^c	Reduced phase ^d	Degree of reduction ^e (%)	TPR (°C)		Degree of oxidation in H ₂ O/He ^f (%)
					Peak 1 Co ₃ O ₄ –CoO	Peak 2 CoO–Co ⁰	
4	24	CoO/Co ₂ SiO ₄	Cubic/hexagonal	65 Co ⁰	297	542	0 (encapsulation)
13	7	Co ₃ O ₄	–	89 Co ⁰	200	326	30
28	3	Co ₃ O ₄	Cubic/hexagonal	98 Co ⁰	166	287	<2

^a Average of TEM and XRD measurements.

^b Dispersion = 96/*d*_{nm}.

^c As observed with XANES. Calcination condition: 250 °C in air.

^d As observed with in situ XRD. Reduction conditions: 425 °C in pure hydrogen.

^e As determined from XANES using a linear combination of reference compounds.

^f Following in situ model oxidation study with XANES at 300–400 °C in H₂O/He (0.04 bar).

sumed to be in a silicate-like phase (35%). Cobalt silicates are known to reduce at temperatures above 800 °C [41].

The spherical model catalysts with large cobalt crystallites (Co-13nm and Co-28nm) were found to be in a well-crystallised Co₃O₄ phase (i.e., after calcination) and to undergo a two-step reduction from Co₃O₄ to CoO and from CoO to Co metal as observed with XRD, TPR, and XANES. Little cobalt silicate was present for these model catalysts (<10% based on the degree of reduction) due to the pH of the impregnation solution (i.e., pH = 3), which minimises the contact and interaction between the cobalt nitrate precursor and silica surface during preparation.

Cobalt crystallite size was also found to affect the reducibility of the spherical Co/SiO₂ model catalysts. With TPR, the reduction of CoO to cobalt metal was found to be strongly dependent on cobalt crystallite size; that is, nanosized (3–4 nm) cobalt crystallites underwent reduction at 540 °C, and the larger (i.e., >8 nm) cobalt crystallites underwent reduction at 287–330 °C (Fig. 14). The need for high temperatures to initiate reduction of the small cobalt oxide crystallites is due to the surface energy of the resulting cobalt crystallites [23] after reduction.

4.2. Influence of cobalt crystallite size on the reduced cobalt phase (i.e., cubic vs. hexagonal cobalt)

The metallic cobalt phase of the spherical Co/SiO₂ model catalysts with large and small cobalt crystallites (i.e., Co-28nm and Co-4nm) were characterised with in situ D-XRD after the samples were reduced. Table 4 summarises the peak heights of the XRD spectra of the spherical Co/SiO₂ model catalysts with large (Co-28nm) and small (Co-4nm) cobalt crystallites compared with the cubic and hexagonal cobalt reference spectra [35].

In the light of the fact that the reduction of the spherical Co/SiO₂ model catalysts were carried out at near the hexagonal-to-cubic phase transition temperature (i.e., 422 °C [43]), one might postulate that this is the reason for the resulting mixture of cubic/hexagonal cobalt. However, with in situ D-XRD, the cubic/hexagonal mixture for the spherical Co/SiO₂ model catalyst with large cobalt crystallites (Co-28nm) was observed at a very low temperature (290 °C), which strongly

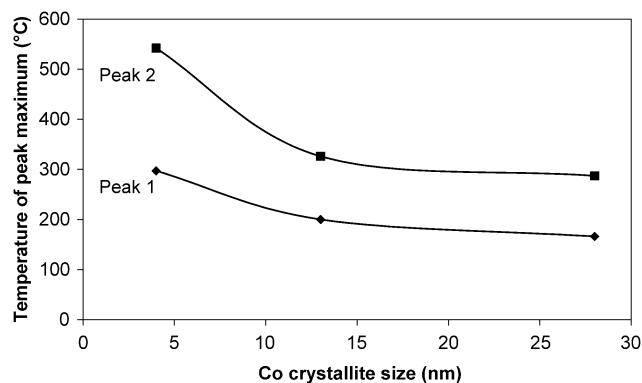


Fig. 14. Influence of cobalt crystallite size on the reducibility of Co₃O₄ to CoO (peak 1) and CoO to Co metal (peak 2) as observed with TPR.

Table 4
Reference intensities for cubic and hexagonal cobalt as compared to the normalised (002) intensities of the spherical model cobalt samples of varying crystallite size (Co-4 and Co-28nm)

Planes (hkl)	hcp [*]	fcc [*]	Co-28nm	Co-4nm
100	44	–	29	–
002	50	100	100	100
101	100	–	32	45
200	–	42	10	28
220	35	23	29	–

* Average of two reference compounds from JCPDS [35].

disproves this hypothesis for this model catalyst. Previous authors have proposed that the cubic/hexagonal mixtures observed for cobalt catalysts are due to the presence of stacking faults [44]. The driving force for these stacking faults is the low energy required for the sliding of the cobalt layers ($E_a = 14$ kJ/mol per Co atom). Smaller cobalt crystallites seem to have more cubic cobalt, as demonstrated by the loss of the hexagonal 100 peak and the increased broadness of the cubic 200 peak. This has been observed for cobalt thin films; that is, the thinner the film, the greater the cubic cobalt phase [45]. Hence, it can be concluded that larger cobalt crystallites (Co-28nm) consist of a faulted mixture of cubic and hexagonal crystallites and that smaller cobalt crystallites (Co-4nm) appear to be more cubic, with a fraction of hexagonal cobalt.

4.3. Comparison of the oxidation behaviour of spherical model catalysts of differing cobalt crystallite size with *in situ* XANES

After reduction, the spherical model catalysts of varying cobalt crystallite sizes were subjected to model oxidation studies ($\text{H}_2\text{O}/\text{He}$). The Co/SiO_2 spherical model catalyst with large cobalt crystallites (Co-28nm) was found to be extremely difficult to oxidise with $\text{H}_2\text{O}/\text{He}$ mixtures up to $P_{\text{H}_2\text{O}} = 0.3$ bar, that is, <5% oxidation at 100 °C. Based on a dispersion of 4% [22], this translates to a surface layer of cobalt oxide assuming similar reactivity of 23 and 45 nm cobalt crystallites. The stability of the large cobalt crystallites (Co-28 nm) is due to the well-faceted (seen clearly in Fig. 6) nature of these crystallites with few defects in the cobalt stacking to aid in the dissociation of water. It has been shown that for nanosized gold crystallites, well-faceted or closed-shell structures are very stable to oxidation by O_2 [46]. The stability of large cobalt crystallites (≥ 28 nm) to oxidation is also often revealed by TEM, which shows a thinner layer of oxide after passivation compared with smaller (<13 nm) cobalt crystallites.

The spherical Co/SiO_2 model catalyst with medium-sized cobalt crystallites (Co-13nm) was found to undergo substantial oxidation (i.e., 30%) at 300 °C in a $\text{H}_2\text{O}/\text{He}$ mixture ($P_{\text{H}_2\text{O}} = 0.04$ bar). Based on a dispersion of 10% [22], this translates into three or four layers of cobalt oxide. The ease of this oxidation is driven by the curvature of cobalt crystallites <13 nm, which have a significant number of defects. The general consensus in the literature is that defects are the preferred sites for dissociation [47] and can explain the higher reactivity of 13 nm cobalt crystallites compared with 28 nm cobalt crystallites. Although this cannot be directly translated to the FTS due to the exclusive use of water as a probe molecule, it gives an indication of the sensitivity of cobalt crystallite size to oxidation and the general difficulties entailed in the oxidation of cobalt with water at these conditions ($P_{\text{H}_2\text{O}} = 0.04\text{--}0.3$ bar, 2–3 h exposure time, 25–300 °C).

The spherical Co/SiO_2 model catalyst with small cobalt crystallites (Co-4nm) was surprisingly found to undergo no surface oxidation under model oxidation conditions ($\text{H}_2\text{O}/\text{He}$, $P_{\text{H}_2\text{O}} = 0.3$ bar, 400 °C), in contradiction to bulk thermodynamics [3]. This was attributed to encapsulation of the small cobalt crystallites with silica as observed with HRTEM. The migration of silica after reduction at temperatures above 500 °C was previously reported for impregnated Co/SiO_2 catalysts [43]. Because this effect was also observed for Co/SiO_2 catalysts prepared by impregnation, the current encapsulation cannot be ascribed to preparation of the model catalyst by precipitation in a strong basic medium.

5. Conclusion

Reasonably well-defined Co/SiO_2 model catalysts with average cobalt crystallite sizes of 4, 13, and 28 nm can be prepared on silica spheres. These spherical model silica catalysts provide optimum and superior TEM characterisation. After calcination, the spherical Co/SiO_2 model catalyst with large cobalt crystal-

lites (i.e., >8 nm) had a well-defined crystalline Co_3O_4 phase, whereas the spherical model catalyst with small cobalt crystallites (4 nm) had an amorphous CoO phase. After reduction, all of the spherical Co/SiO_2 model catalysts were found to contain a mixture of fcc and hcp cobalt. The spherical Co/SiO_2 model catalyst with small cobalt crystallites (4 nm) did not oxidize in $\text{He}/\text{H}_2\text{O}$ model environments ($P_{\text{H}_2\text{O}} = 0.3$ bar, 400 °C), due to encapsulation of the metallic cobalt with silica after reduction. The spherical Co/SiO_2 model catalyst with medium-sized (i.e., 13 nm) cobalt crystallites underwent oxidation at 100 °C and reached a maximum oxidation of 30% at 300 °C. The oxidation was limited to three or four layers of the surface of the cobalt crystallites. The spherical Co/SiO_2 model catalysts with large (i.e., 28 nm) cobalt crystallites underwent very little oxidation (i.e., <2%) at 300 °C. In general, it was found that the oxidation of spherical Co/SiO_2 model catalysts with water is difficult and size-dependent.

Acknowledgments

The authors thank M. Claeys for assisting with catalyst preparation, C.P.J. Verhagen for introducing the preparation of silica spheres, and B. Breedt and J.J. Retief for assisting with D-XRD measurements.

References

- [1] Gas-to-liquids: Peering into the crystal ball, The Catalyst Review Newsletter, April (2005), p. 4.
- [2] E. Iglesia, Appl. Catal. A: Gen. 161 (1997) 59.
- [3] P.J. van Berge, J. van de Loosdrecht, S. Barradas, A.M. van der Kraan, Catal. Today 58 (2000) 321.
- [4] B. Eisberg, R.A. Fiato, Stud. Surf. Sci. Catal. 199 (1998) 961.
- [5] M.M. G Senden, A.D. Punt, A. Hoek, Stud. Surf. Sci. Catal. 199 (1998) 943.
- [6] M.E. Dry, Catal. Today 71 (2002) 227.
- [7] E. Iglesia, S.L. Soled, R.A. Fiato, J. Catal. 137 (1992) 212.
- [8] S.W. Ho, M. Houalla, D.M. Hercules, J. Phys. Chem. 94 (1990) 6396.
- [9] D. Schanke, A.M. Hilmen, E. Bergene, K. Kinnari, E. Rytter, E. Ådnanes, A. Holmen, Catal. Lett. 34 (1995) 269.
- [10] D. Schanke, A.M. Hilmen, E. Bergene, K. Kinnari, E. Rytter, E. Ådnanes, A. Holmen, Energy Fuels 10 (1996) 867.
- [11] M. Rothaemel, K.F. Hanssen, E.A. Blekkan, D. Schanke, A. Holmen, Catal. Today 38 (1997) 79.
- [12] M.W.J. Craje, A.M. van der Kraan, J. van de Loosdrecht, P.J. van Berge, Catal. Today 71 (2002) 369.
- [13] G. Jacobs, T.K. Das, P.M. Patterson, J. Li, L. Sanchez, B.H. Davis, Appl. Catal. A: Gen. 253 (2003) 8553.
- [14] G. Jacobs, P.M. Patterson, Y. Zhang, T.K. Das, J. Li, B.H. Davis, Appl. Catal. A: Gen. 233 (2002) 215.
- [15] G. Kiss, C.E. Kliever, G.J. DeMartin, C.C. Culross, J.E. Baumgartner, J. Catal. 217 (2003) 127.
- [16] E. Iglesia, Stud. Surf. Sci. Catal. 107 (1997) 153.
- [17] J. van de Loosdrecht, P.J. van Berge, M.W.J. Craje, A.M. van der Kraan, Hyperfine Interact. 139/140 (2002) 3.
- [18] T.K. Das, G. Jacobs, P.M. Patterson, W.A. Conner, J. Li, B.H. Davis, Fuel 82 (2003) 805.
- [19] J. Li, X. Zhan, Y. Zhang, G. Jacobs, T. Das, B.H. Davis, Appl. Catal. A: Gen. 228 (2002) 203.
- [20] G. Jacobs, Y. Zhang, T.K. Das, P.M. Patterson, B.H. Davis, Stud. Surf. Sci. Catal. 139 (2001) 415.
- [21] S. Storæter, Ø. Borg, E.A. Blekkan, A. Holmen, J. Catal. 231 (2005) 405.

- [22] F.M. Gottschalk, R.G. Copperthwaite, M. van der Riet, G.J. Hutchings, *Appl. Catal. A: Gen.* 38 (1988) 103.
- [23] E. van Steen, M. Claeys, M. Dry, E. Viljoen, J. van de Loosdrecht, J.L. Visagie, *J. Phys. Chem. B* 109 (2005) 3575.
- [24] P.J. van Berge, J. van de Loosdrecht, J.L. Visagie, US Patent 6,385,690 (2004), to Sasol.
- [25] C.J. Kim, European Patent 0339923 A1 (1989), to Exxon.
- [26] C.J. Kim, US Patent 5,227,407 (1993), to Exxon.
- [27] G.P. Huffman, N. Shah, J. Zhao, F.E. Huggins, T.E. Hoost, S. Halvorsen, G.J. Goodwin, *J. Catal.* 151 (1995) 17.
- [28] H. Schulz, E. van Steen, M. Claeys, *Stud. Surf. Sci. Catal.* 81 (1994) 455.
- [29] A.K. Datye, N.J. Long, *Ultramicroscopy* 25 (1988) 203.
- [30] S. Chakraborti, A.K. Datye, N.J. Long, *J. Catal.* 108 (1987) 444.
- [31] W. Stober, A. Fink, E. Bohn, *J. Colloid Interface Sci.* 26 (1968) 62.
- [32] M. Roy, B. Didillon, D. Uzio, US Patent 6,214,890 (1999), to IFP.
- [33] D. Schanke, S. Vada, E.A. Blekkan, A.M. Hilmen, A. Hoff, A. Holmen, *J. Catal.* 155 (1995) 85.
- [34] R.D. Jones, C.H. Bartholomew, *Appl. Catal.* 39 (1988) 77.
- [35] W.F. McClune (Ed.), *Powder Diffraction Files*, International Centre for Diffraction Data, Pennsylvania, USA, 1996.
- [36] P. Scherrer, *Gott. Nachr.* 2 (1918) 98.
- [37] <http://www.csriiit.edu/periodic-table.html>.
- [38] F.W. Lytle, R.B. Gregor, E.C. Marques, D.R. Sansrom, G.H. Via, J.H. Sinfelt, *J. Catal.* 95 (1985) 546.
- [39] F.W. Lytle, P.S.P. Wei, R.B. Gregor, G.H. Via, J.H. Sinfelt, *J. Chem. Phys.* 70 (1979) 4849.
- [40] G. Mestl, H. Knozinger, in: G. Ertl, H. Knozinger, J. Weitkamp (Eds.), *Handbook of Heterogeneous Catalysis*, vol. 2, Wiley-VCH, Weinheim, 1997, p. 539.
- [41] E. van Steen, G.S. Sewell, R.A. Makhothe, C. Mickelthwaite, H. Manstein, M. de Lange, C.T. O'Connor, *J. Catal.* 162 (1996) 220.
- [42] A. Barbier, A. Hanif, J.A. Dalmon, G.A. Martin, *Appl. Catal. A: Gen.* 168 (1998) 333.
- [43] J.M. Jablonski, J. Okal, D. Potoczna-Petru, L. Krajczyk, *J. Catal.* 220 (2003) 146.
- [44] V.F. Puentes, K.M. Krishnan, A.P. Alivisatos, *Science* 291 (2001) 2115.
- [45] M. Hecker, N. Mattern, W. Bruckner, C.M. Schneider, *Mater. Sci. Forum* 243 (2004) 193.
- [46] H.-G. Boyen, G. Kastel, F. Weigl, B. Koslowski, C. Dietrich, P. Ziemann, J.P. Spatz, S. Riethmuller, C. Hartmann, M. Moller, G. Schmid, M.G. Garnier, P. Oelhafen, *Science* 297 (2002) 1533.
- [47] X.-Q. Gong, R. Raval, P. Hu, *Surf. Sci.* 562 (2004) 247.